Safety and Efficacy of Transcranial Direct Current Stimulation in Acute Experimental Ischemic Stroke

Luca Peruzzotti-Jametti, Marco Cambiaghi, Marco Bacigaluppi, Mattia Gallizioli, Edoardo Gaude, Silvia Mari, Stefano Sandrone, Marco Cursi, Luis Teneud, Giancarlo Comi, Giovanna Musco, Gianvito Martino and Letizia Leocani

Stroke. published online August 27, 2013;
Stroke is published by the American Heart Association, 7272 Greenville Avenue, Dallas, TX 75231

Print ISSN: 0039-2499. Online ISSN: 1524-4628

Original Contribution

Safety and Efficacy of Transcranial Direct Current Stimulation in Acute Experimental Ischemic Stroke

Luca Peruzzotti-Jametti, MD*; Marco Cambiaghi, PhD*; Marco Bacigaluppi, MD, PhD; Mattia Gallizioli, MSc; Edoardo Gaude, MSc; Silvia Mari, PhD; Stefano Sandrone; Marco Cursi, Eng; Luis Teneud, MD, PhD; Giancarlo Comi, MD; Giovanna Musco, PhD; Gianvito Martino, MD*; Letizia Leocani, MD, PhD*

Background and Purpose—Transcranial direct current stimulation is emerging as a promising tool for the treatment of several neurological conditions, including cerebral ischemia. The therapeutic role of this noninvasive treatment is, however, limited to chronic phases of stroke. We thus ought to investigate whether different stimulation protocols could also be beneficial in the acute phase of experimental brain ischemia.

Methods—The influence of both cathodal and anodal transcranial direct current stimulation in modifying brain metabolism of healthy mice was first tested by nuclear magnetic resonance spectroscopy. Then, mice undergoing transient proximal middle cerebral artery occlusion were randomized and treated acutely with anodal, cathodal, or sham transcranial direct current stimulation. Brain metabolism, functional outcomes, and ischemic lesion volume, as well as the inflammatory reaction and blood brain barrier functionality, were analyzed.

Results—Cathodal stimulation was able, if applied in the acute phase of stroke, to preserve cortical neurons from the ischemic damage, to reduce inflammation, and to promote a better clinical recovery compared with sham and anodal treatments. This finding was attributable to the significant decrease of cortical glutamate, as indicated by nuclear magnetic resonance spectroscopy. Conversely, anodal stimulation induced an increase in the postischemic lesion volume and augmented blood brain barrier derangement.

Conclusions—Our data indicate that transcranial direct current stimulation exerts a measurable neuroprotective effect in the acute phase of stroke. However, its timing and polarity should be carefully identified on the base of the pathophysiological context to avoid potential harmful side effects. **(*Stroke*. 2013;44:00-00.)**

Key Words: electric stimulation ■ mice ■ neuroprotective agents ■ stroke

Transcranial direct current stimulation (tDCS) is currently used to modulate brain activity in many neurological disorders.[1] Several tDCS approaches, based on different polarity, density of current, and timing of application, have been proposed.[2] In stroke patients, the ability of tDCS to modulate cortical activity of both the lesioned and the unaffected hemisphere has been used, so far, to ameliorate chronic motor impairment, poststroke depression, and cortical deficits.[3] Anodal stimulation (A-tDCS) of the affected hemisphere or cathodal stimulation (C-tDCS) of the unaffected hemisphere are currently used in stroke clinical trials with the main aim of increasing synaptic plasticity by counteracting the functional imbalance between the 2 hemispheres.[4] In earlier phases of stroke, the use of tDCS is still controversial and has shown some hints of efficacy. Excitatory A-tDCS improved motor performances if applied 2 days after permanent ischemic stroke in rats,[5] whereas inhibitory electric stimulation produced slight positive effects in a model of transient ischemia.[6] The effects of tDCS in acute stroke are, therefore, far from being fully understood and a finetuning of the technique, based on the pathological context and timing, is still mandatory to foster bench-to-bedside translation.[7] Among the proposed mechanisms of action of tDCS,[8] it is known that A-tDCS is able to increase neuronal excitability and spontaneous firing, whereas C-tDCS has opposite effects.[9,10] In fact, C-tDCS in healthy humans reduces neurotransmitters, such as gamma-aminobutyric acid (GABA) and glutamate, exerting an inhibitory effect.[11] Interestingly, a therapeutic tDCS protocol in acute stroke could limit the massive

Received April 4, 2013; final revision received July 15, 2013; accepted July 23, 2013.

From the Neuroimmunology Unit (L.P.-J., M.B., M.G., S.S., G.C., G.M.) and Experimental Neurophysiology Unit, Division of Neuroscience, Institute of Experimental Neurology (INSPE), DIBIT-II, San Raffaele Scientific Institute (M.C., M.C., L.T., G.C., L.L.), Vita-Salute San Raffaele University, Milan, Italy; and Dulbecco Telethon Institute, Biomolecular NMR Laboratory c/o Center for Translational Genomics and Bioinformatics, Ospedale San Raffaele, Milan, Italy (E.G., S.M., G.M.).

*Drs Peruzzotti-Jametti, Cambiaghi, Martino, and Leocani contributed equally.

The online-only Data Supplement is available with this article at http://stroke.ahajournals.org/lookup/suppl/doi:10.1161/STROKEAHA.113.001687/-/DC1.

Correspondence to Gianvito Martino, MD, or Letizia Leocani, MD, PhD, San Raffaele Scientific Institute, Via Olgettina 58, 20132 Milan, Italy. E-mail martino.gianvito@hsr.it or letizia.leocani@hsr.it

Stroke **is available at http://stroke.ahajournals.org** **DOI: 10.1161/STROKEAHA.113.001687**

release of excitatory neurotransmitters from damaged neurons, among which glutamate exerts a pivotal role in triggering early excitotoxic damage and cortical spreading depression waves.[12] We, therefore, investigated whether the application of tDCS would exert overall inhibitory effects in the acute phase of stroke, thus limiting the ischemic damage and avoiding functional disability.

Materials and Methods

Animals and Experimental Procedures

This study was performed on a total of 137 C57BL/6 male mice purchased from Charles River Italy and aged 8 to 10 weeks (20–22 g).

A group of 36 healthy mice underwent sham middle cerebral artery occlusion (MCAO) coupled with a tDCS protocol consisting of 20′ on–20′ off–20′ on of either cathodal tDCS (C-tDCS-sham) or anodal tDCS (A-tDCS-sham), and the control group remained nonstimulated (N-tDCS-sham; Figure IA in the online-only Data Supplement). These healthy mice were euthanized for nuclear magnetic resonance (NMR) spectroscopy (C-tDCS-sham n=4; A-tDCS-sham n=4; N-tDCS-sham n=4) and Western blot analysis (C-tDCS-sham n=8; A-tDCS-sham n=8; N-tDCS-sham n=8) immediately after tDCS.

In order to test the effects of tDCS on cerebral ischemia, 101 mice were weighted and randomized into 3 treatment groups and subjected to 90-minute-long proximal MCAO.

Mice (n=75) were treated with the same tDCS protocol consisting of 20′ on–20′ off–20′ on of either cathodal tDCS (C-tDCS-MCAO n=25) or anodal tDCS (A-tDCS-MCAO n=25), and the control group remained nonstimulated (N-tDCS-MCAO n=25) starting after the first 30 minutes of MCAO (Figure IC in the online-only Data Supplement). Regional cerebral blood flow (rCBF) was calculated during MCAO and following reperfusion. A randomly selected subgroup of 9 ischemic mice was euthanized for NMR, immediately after the procedure (N-tDCS-MCAO n=3; C-tDCS-MCAO n=3; A-tDCS-MCAO n=3). Forty-three ischemic mice were weighted and euthanized for histological analysis at 24 hours (C-tDCS-MCAO n=17; A-tDCS-MCAO n=17; N-tDCS-MCAO n=18) and a subgroup of 18 animals (N-tDCS-MCAO n=6; C-tDCS-MCAO n=6; A-tDCS-MCAO n=6) was randomly selected for neurophysiological and behavioral functional assessment prior to enthanization.

Twenty-three ischemic mice were allowed to survive ≤72 hours after ischemia (C-tDCS-MCAO n=8; A-tDCS-MCAO n=8; N-tDCS-MCAO n=7) to estimate final lesion volume, pathology, and behavior.

In another experimental stimulation setup, mice (n=26) were subjected to 90-minute-long proximal MCAO and were treated with the same tDCS protocol consisting of 20′ on–20′ off–20′ on starting 4.5 hours after the induction of MCAO (C-tDCS-MCAO n=8; A-tDCS-MCAO n=8; N-tDCS-MCAO n=10; Figure II in the online-only Data Supplement). Overall mortality rate was 25% (8/32) in N-tDCS-MCAO, 6.7% (2/30) in C-tDCS-MCAO, and 20% (6/30) in A-tDCS-MCAO group.

Experimental procedures were approved by the Institutional Animal Care and Use Committee at San Raffaele Scientific Institute. All animals and results were studied in a blinded fashion for treatment. For detailed description of abovementioned techniques, see online-only Data Supplement.

Results

tDCS Modifies Metabolite Pattern and N-Methyl-D-Aspartate Receptor Expression in Healthy Mouse Cortex

To first investigate the metabolic effect of tDCS, C57BL/6 healthy mice were subjected to either sham, cathodal, or anodal t-DCS with a protocol consisting of 20′ on–20′ off–20′ on stimulation. According to previous literature[13] and pilot experiments (Figure III in the online-only Data Supplement), we identified this stimulation protocol as the best suited to induce long-term results (repeated stimulation based on priming effect) without inducing current-related tissue damage (short stimulation periods). Immediately after stimulation, we measured a wide range of metabolic cortical patterns by NMR spectroscopy (Figure 1B). C-tDCS-treated healthy mice (hereafter referred as C-tDCS-sham) showed a significant decrease in cortical glutamate compared with nonstimulated sham–treated healthy mice (N-tDCS-sham; ratio 0.75; $P<0.05$). A statistically significant decrease of alanine levels was also observed in the cortex of C-tDCS-sham, when compared with A-tDCS-treated healthy mice (A-tDCS-sham; ratio 0.68; $P<0.05$). A-tDCS-sham mice displayed instead an increase of cortical lactate compared with N-tDCS-sham mice (ratio 1.258; $P<0.05$; Figure 1A).

To validate whether glutamatergic synaptic transmission was effectively altered by C-tDCS, we measured by Western blot analysis the expression of 2 NMDA receptor (NMDAR) subunits: NR1 and NR2B. The former subunit is constitutively expressed, whereas the latter exerts a regulatory function during increased glutamatergic transmission.[14]

Although there were no differences in the expression of NR1 subunit among the 3 groups, C-tDCS-sham mice displayed a statistically significant lower expression of the NR2B subunit compared with both N-tDCS-sham ($P<0.05$) and A-tDCS-sham mice ($P<0.05$; Figure 1C). Altogether, these results indicate that C-tDCS, but not A-tDCS, is able to reduce cortical glutamate activity and metabolism.

C-tDCS Protects From Ischemic Brain Damage

In order to investigate the role of tDCS in acute stroke, we applied the identified stimulation protocol (20′ on–20′ off–20′ on) to C57BL/6 mice in the very acute phase of 90-minute-long transient proximal MCAO (Figure IC in the online-only Data Supplement).

Mean weight loss at 24 hours over baseline was comparable among the 3 treatment groups (−8.5%±1.5 SEM in N-tDCS-MCAO; −12.4%±1.2 SEM in C-tDCS-MCAO; and −10.9%±0.9 SEM in A-tDCS-MCAO), whereas modified Neurological Severity Score revealed a significant treatment effect ($H=8.65$; 2 d.f.; $P<0.05$) with an amelioration induced by C-tDCS compared with N-tDCS-MCAO and A-tDCS-MCAO mice ($P<0.05$) that persisted ≤3 days after ischemia ($H=7.60$; 2 d.f.; $P<0.05$; Figure 2A). We also performed a functional neurophysiological assessment of resting motor threshold (RMT) by stimulating the cortex of ischemic mice at 24 hours postischemia. RMT displayed a significant treatment effect and C-tDCS-MCAO mice had a preservation of RMT compared with A-tDCS-MCAO and N-tDCS-MCAO mice ($H=7.89$; 2 d.f.; $P<0.05$). RMT did not significantly increase over baseline in C-tDCS-MCAO mice (baseline values, 4.13±0.24 SEM; 24-hour values, 4.53±0.44 SEM; increase over baseline, 109.0%±6.73 SEM; n.s.), whereas it significantly increased in both A-tDCS-MCAO (baseline values, 4.37±0.20 SEM; 24-hour values, 6.37±0.50 SEM; increase over baseline, 159.9%±12.45 SEM; $P<0.001$) and N-tDCS-MCAO mice (baseline values, 4.25±0.19 SEM; 24-hour values, 6.32±0.41 SEM; increase over baseline, 150.5%±12.32 SEM; $P<0.001$). These findings were supportive of a

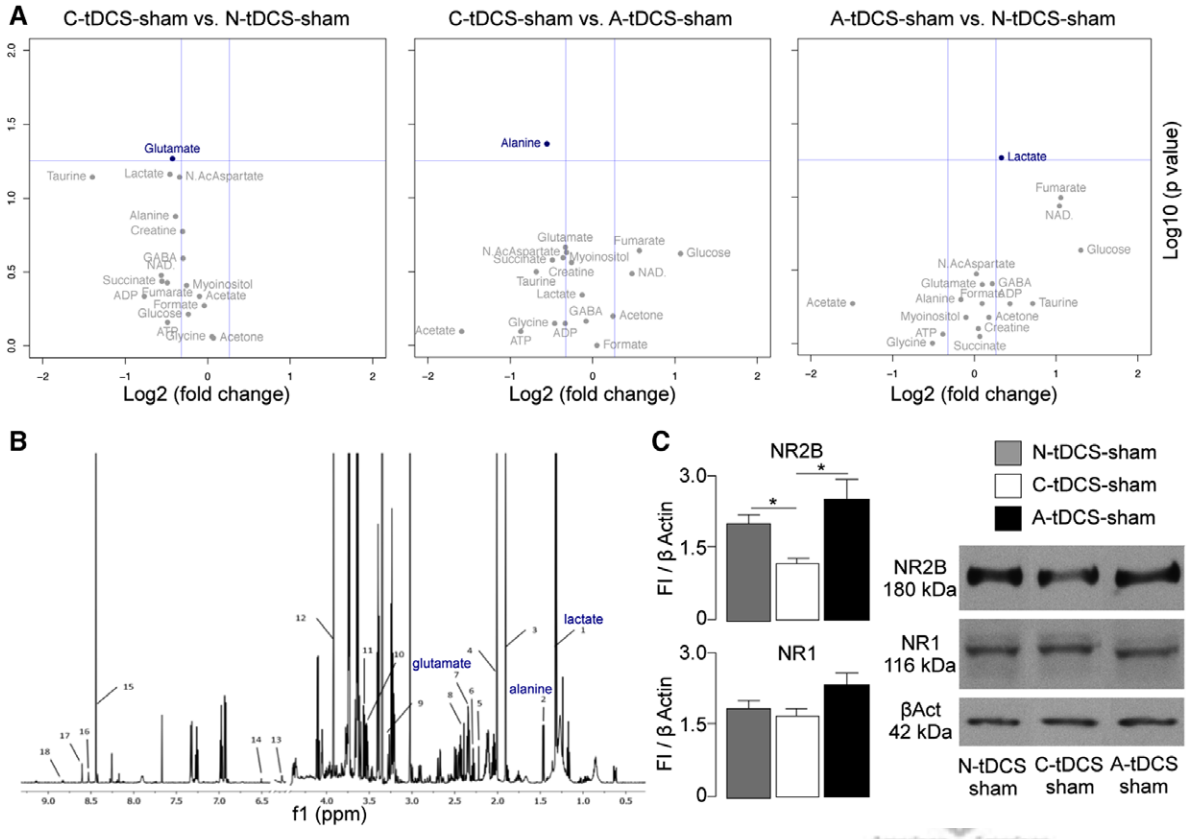

Figure 1. Transcranial direct current stimulation modifies cortical metabolites and NMDA (N-methyl-D-aspartate) receptor expression in healthy mice. **A**, Cortical metabolites were evaluated by nuclear magnetic resonance spectroscopy on brains of healthy mice euthanized immediately after transcranial direct current stimulation (tDCS); volcano plots comparing the 3 groups were then analyzed. C-tDCS (cathodal tDCS) induced a reduction of total glutamate compared with N-tDCS-sham (nonstimulated) mice and a reduction of alanine compared with A-tDCS-sham (anodal) mice. A-tDCS led to a significant increase of cortical lactate compared with N-tDCS-sham mice. Data are plotted as Log2 of fold changes over –Log10 of *P* values. Variables in blue are significant ($P<0.05$) and show fold changes >1.2 or <0.8. **B**, Identification of metabolites in 1D-1H-noesy spectrum of a cortical extract (1: lactate, 2: alanine, 3: acetate, 4: N-acetyl aspartate, 5: acetone, 6: gamma-aminobutyric acid (GABA), 7: glutamate, 8: succinate, 9: taurine, 10: myoinositol, 11: glycine, 12: creatine, 13: glucose, 14: fumarate, 15: formate, 16: ADP, 17: ATP, 18: NAD^+). **C**, Expression of NR1 and NR2B subunits of the NMDA receptor from the cortex of tDCS-sham mice. Although no differences in NR1 protein level were found among the 3 groups, NR2B was significantly decreased in C-tDCS-sham mice (white bars), compared with N-tDCS-MCAO (grey bars) and A-tDCS-MCAO mice (black bars). Error bars in all panels indicate SEM, *$P<0.05$.

neuroprotective role of C-tDCS on the ischemic sensorimotor area and corticospinal tract.

Neuropathological analysis revealed indeed that C-tDCS induced a specific preservation of the cytoarchitecture of the cerebral cortex, a feature never observed in N-tDCS-MCAO and A-tDCS-MCAO mice (Figure 2B). Stereological morphometric analysis of the ischemic lesion volume confirmed a significant treatment effect ($F_{2,33}=20.40$; $P<0.0001$). C-tDCS-MCAO mice showed a remarkable reduced ischemic volume (34.18%±2.37 SEM) compared with both N-tDCS-MCAO (54.22%±2.30 SEM; $P<0.001$) and A-tDCS-MCAO mice (47.29%±2.77 SEM; $P<0.001$). Although the reduction of infarct volume in C-tDCS-MCAO mice persisted over time (30.46%±2.10 SEM; $P<0.01$ versus N-tDCS-MCAO, and $P<0.001$ versus A-tDCS-MCAO), at 3 days postischemia A-tDCS-MCAO mice showed an increased ischemic lesion (58.67%±2.59 SEM) compared with N-tDCS-MCAO mice (48.13%±1.25 SEM; $P<0.01$; Figure 2C). At the same time point, a reduction of brain edema was also observed in C-tDCS-MCAO (17.52%±2.64 SEM) compared with N-tDCS-MCAO (32.23%±2.13 SEM; $P<0.01$) and A-tDCS-MCAO mice (26.80%±1.13 SEM; $P<0.01$). Consistently, quantification of apoptotic cells in cortical and striatal areas, identified as activated $Caspase3^+$ cells, displayed a significant treatment effect ($H=18.17$; 2 d.f.; $P<0.001$, and $H=10.87$; 2d.f.; $P<0.01$, respectively): at cortical and striatal level, C-tDCS-MCAO mice had a reduced number of $Caspase3^+$ cells compared with both N-tDCS-MCAO ($P<0.05$) and A-tDCS-MCAO ($P<0.01$). Indeed, apoptosis of cortical neurons ($Casp3^+NeuN^+$ cells) was reduced in C-tDCS-MCAO (0.37±0.07 SEM) compared with both N-tDCS-MCAO (1.69±0.36 SEM) and A-tDCS-MCAO mice (2.4±0.33 SEM; $P<0.05$). On the contrary, A-tDCS-MCAO mice had a significant increase in the number of apoptotic cells compared with N-tDCS-MCAO mice ($P<0.05$) with an increased number of both apoptotic neurons and endothelial cells.

We further investigated whether the clinicopathological protective effect of C-tDCS in MCAO mice was preceded by an alteration of cortical metabolites. NMR metabolic profiles were assessed in all treatment groups: C-tDCS-MCAO mice showed a significant decrease of cortical glutamate (ratio 0.53; $P<0.05$) in comparison with N-tDCS-MCAO mice.

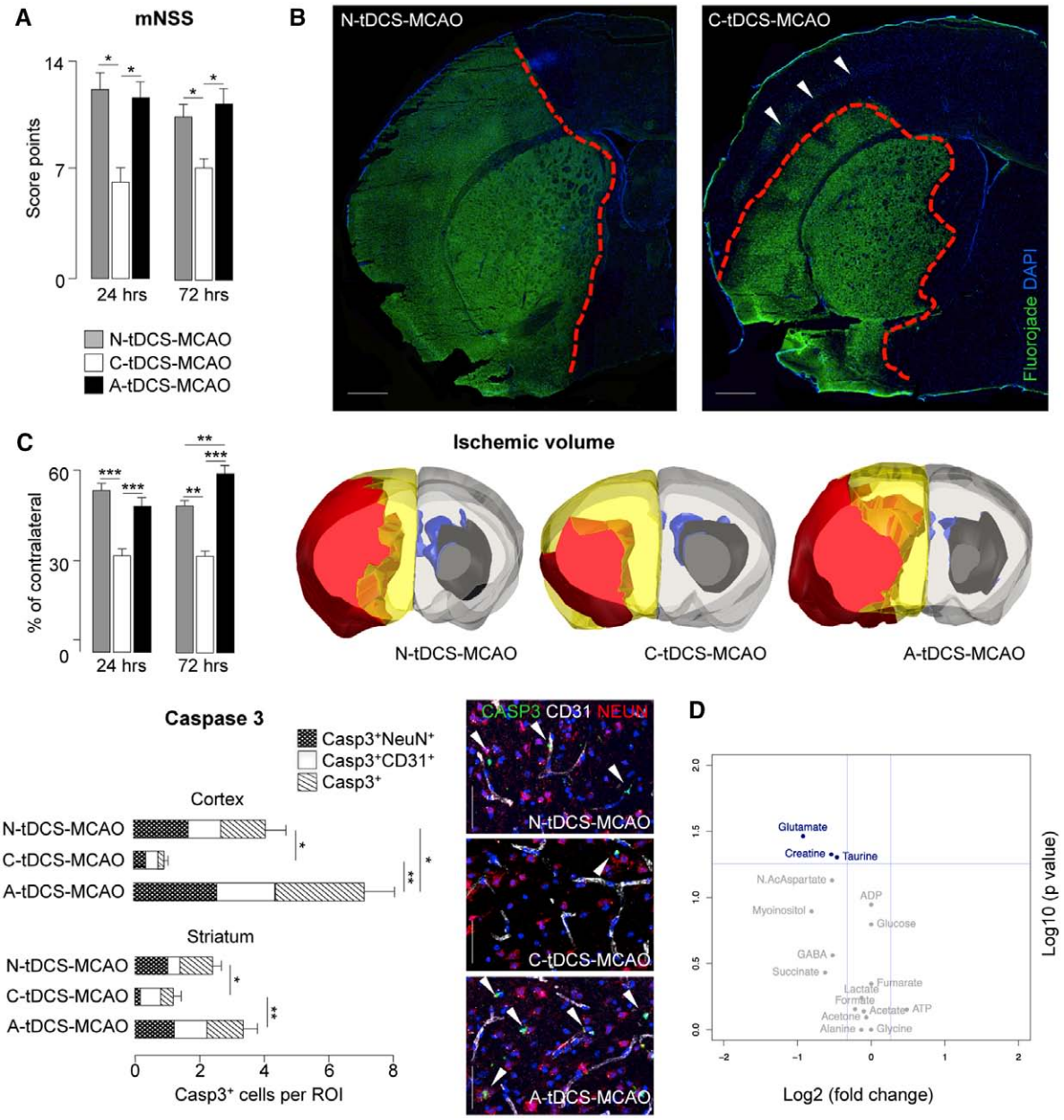

Figure 2. Cathodal transcranial direct current stimulation (C-tDCS) ameliorates functional deficits and reduces ischemic damage in middle cerebral artery occlusion (MCAO) mice. **A**, C-tDCS-MCAO mice (white bars) showed less disability at 24 and 72 hours postischemia, evaluated with the modified Neurological Severity Score (mNSS), compared with both N-tDCS-MCAO (nonstimulated; gray bars) and A-tDCS-MCAO (anodal; black bars) mice. **B**, Representative brain sections of a N-tDCS-MCAO mouse and a C-tDCS-MCAO mouse, stained with Fluoro-Jade-B (green). Preservation of the cortex from the ischemic damage (arrowheads) is observed in the C-tDCS-MCAO mouse. Red dashed lines represent the ischemic border. Nuclei are counterstained with DAPI (4′-6-diamidino-2-phenylindole; blue). Scale bars, 500 μm. **C**, C-tDCS reduced final ischemic volume and apoptosis in treated mice. Serial 3-dimensional reconstructions of the ischemic volume at 24 hours after MCAO showed a great reduction of the ischemic lesion in C-tDCS-MCAO mice. A representative mouse from each group is shown: note the contralateral healthy hemisphere (gray), contralateral healthy striatum (black), contralateral ventricles (blue), ipsilateral ischemic lesion (red), and nonlesioned ipsilateral tissue (yellow). C-tDCS-MCAO mice displayed also a significant reduction of the number of Caspase3$^+$ cells (arrowheads) compared with A-tDCS-MCAO and N-tDCS-MCAO mice, both in the cortex and in the striatum at 24 hours. Particularly, C-tDCS significantly reduced the number of cortical Caspase3$^+$NeuN$^+$ cells compared with other treatments. Notably, A-tDCS-MCAO mice showed an increased total number of cortical Caspase3$^+$ cells compared with N-tDCS-MCAO mice. Representative Caspase3 (green), NeuN (red), and CD31 (white) staining of the ischemic cortex are shown. Nuclei are counterstained with DAPI (4′-6-diamidino-2-phenylindole; blue). Scale bars, 50 μm. **D**, Nuclear magnetic resonance spectroscopy and Volcano plot comparing cortical metabolites of C-tDCS-MCAO and N-tDCS-MCAO mice. A significant reduction of total glutamate, creatine, and taurine was found in the ischemic cortex of C-tDCS-MCAO mice. Data are plotted as Log2 of fold changes over –Log10 of *P* values. Metabolites depicted in blue are significantly changed ($P<0.05$) and show fold changes >1.2 or <0.8. Error bars in all panels indicate SEM, $^*P<0.05$, $^{**}P<0.01$, $^{***}P<0.001$.

In addition, creatine (ratio 0.69; $P<0.05$) and taurine (ratio 0.72; $P<0.05$) levels were reduced in C-tDCS MCAO mice (Figure 2D), confirming the overall inhibitory activity of C-tDCS on ischemic brain metabolism.

Inflammatory Response in MCAO Mice Treated by tDCS

In order to investigate the mechanisms underlying the effects of tDCS on MCAO mice, we evaluated the periischemic inflammatory response, namely resident ionized calcium-binding adapter molecule 1 (Iba1)$^+$ microglia, blood-borne CD45$^+$ central nervous system-infiltrating mononuclear cells, and myeloperoxidase (MPO)$^+$ neutrophils, at 24 and 72 hours postischemia.

No difference in the number of Iba1$^+$ cells was found at striatal level, whereas there was a striking difference at cortical level among the 3 treatment groups at 24 hours postischemia ($H=9.62$; 2 d.f.; $P<0.01$); a lower amount of Iba1$^+$ cells was found in the periischemic cortex of C-tDCS-MCAO mice, compared with both N-tDCS-MCAO and A-tDCS-MCAO mice ($P<0.05$; Figure 3A–3C).

Quantification of periischemic CD45$^+$ leucocytes showed also a significant treatment effect both in the periischemic cortex and striatum ($H=9.673$; 2 d.f.; $P<0.01$, and $H=6.140$; 2 d.f.; $P<0.05$). A-tDCS-MCAO mice presented increased numbers of periischemic CD45$^+$ cells compared with both C-tDCS-MCAO (cortex, $P<0.05$ at 24 and 72 hours; striatum, $P<0.01$ at 72 hours) and N-tDCS-MCAO mice (striatum $P<0.05$ at 24 and 72 hours; cortex $P<0.05$ at 72 hours; Figure 3B and 3C). Similarly, MPO$^+$ neutrophils in the upper ischemic cortex and striatum showed a significant treatment effect at 24 ($H=9.27$; 2 d.f.; $P<0.01$, and $H=8.92$; 2 d.f.; $P<0.05$, respectively) and 72 hours postischemia ($H=5.87$; 2 d.f.; $P<0.05$, and $H=4.86$; 2 d.f.; $P<0.05$, respectively): A-tDCS-MCAO mice showed a significant increase of infiltrating MPO$^+$ cells with respect to both N-tDCS-MCAO (upper cortex, $P<0.05$; striatum, $P<0.01$) and C-tDCS-MCAO mice (upper cortex, $P<0.01$; striatum, $P<0.05$) 24 hours postischemia (Figure 3D). Interestingly, although MPO$^+$ and CD45$^+$ cells augmented in the cortex of N-tDCS-MCAO mice at 72 hours postischemia, C-tDCS-MCAO mice had a lower number of infiltrating cells compared with A-tDCS-MCAO mice ($P<0.05$).

A-tDCS Exacerbates Dysregulation of Postischemic Blood Brain Barrier

The increased number of inflammatory cells in A-tDCS-MCAO mice prompted us to investigate whether this stimulation protocol might have provoked a further dysregulation of the postischemic blood brain barrier (BBB). We thus evaluated the ratio of endogenous IgG extravasation in the ipsilateral ischemic over the contralateral healthy hemisphere (Figure 4A). A significant treatment effect was found ($H=9.49$; 2 d.f.; $P<0.01$, $H=9.18$; 2 d.f.; $P<0.05$, and $H=7.96$; 2 d.f.; $P<0.05$, respectively). A-tDCS-MCAO mice showed a significant increase of endogenous IgG leakage with respect to N-tDCS-MCAO (upper cortex, $P<0.05$) and C-tDCS-MCAO

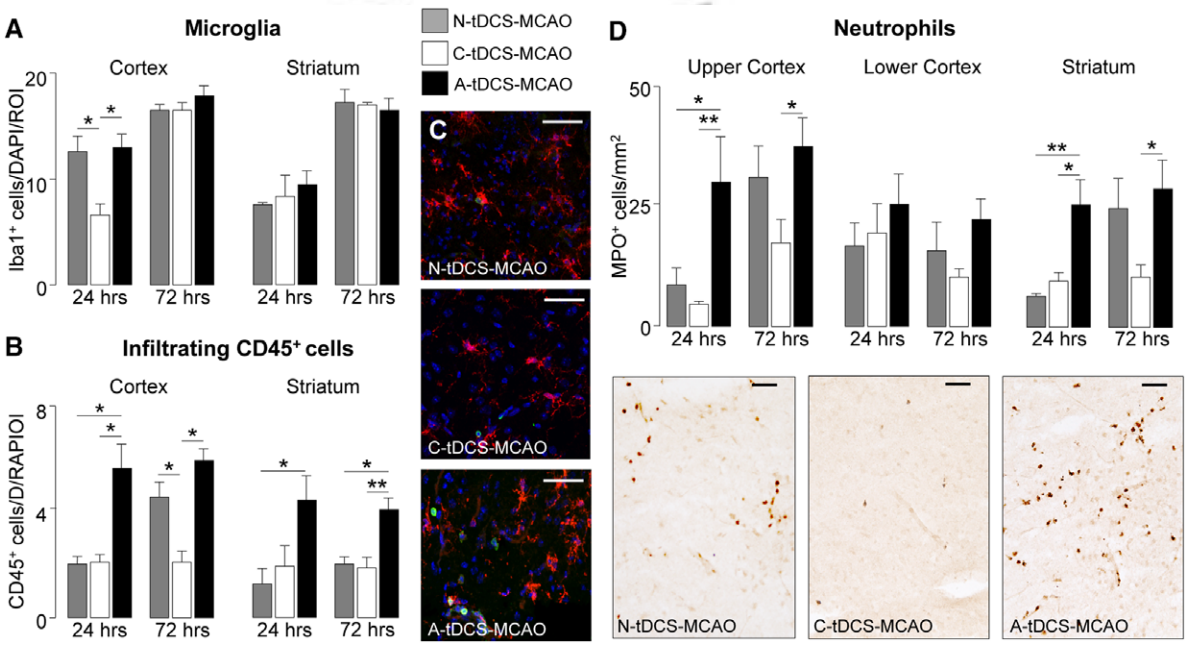

Figure 3. Periischemic inflammatory response is altered by transcranial direct current stimulation (tDCS). **A**, Mice that underwent cathodal tDCS middle cerebral artery occlusion (C-tDCS-MCAO; white bars) displayed a lower number of ionized calcium-binding adapter molecule 1 (Iba1)$^+$ cells in the periischemic cortex compared with both N-tDCS-MCAO (nonstimulated; gray bars) and A-tDCS-MCAO (anodal; black bars) mice at 24 hours postischemia. **B**, A-tDCS-MCAO mice showed instead a significant increase of CD45$^+$ cells in the periischemic cortex and striatum, compared with C-tDCS-MCAO and N-tDCS-MCAO mice that persisted ≤72 hours postischemia. **C**, Representative images of periischemic cortical Iba1$^+$ (red) and CD45$^+$ cells (green) at 24 hours postischemia. Nuclei are counterstained with DAPI (4′-6-diamidino-2-phenylindole; blue). Scale bars, 50 μm. **D**, A-tDCS-MCAO mice were characterized by a significant increase of myeloperoxidase (MPO)$^+$ cells in the upper cortex and striatum, compared with C-tDCS-MCAO and N-tDCS-MCAO mice. Representative images of MPO$^+$ neutrophils (brown) in the upper cortex of treated mice at 24 hours postischemia. Scale bars, 50 μm. Error bars in all panels indicate SEM, *$P<0.05$, **$P<0.01$.

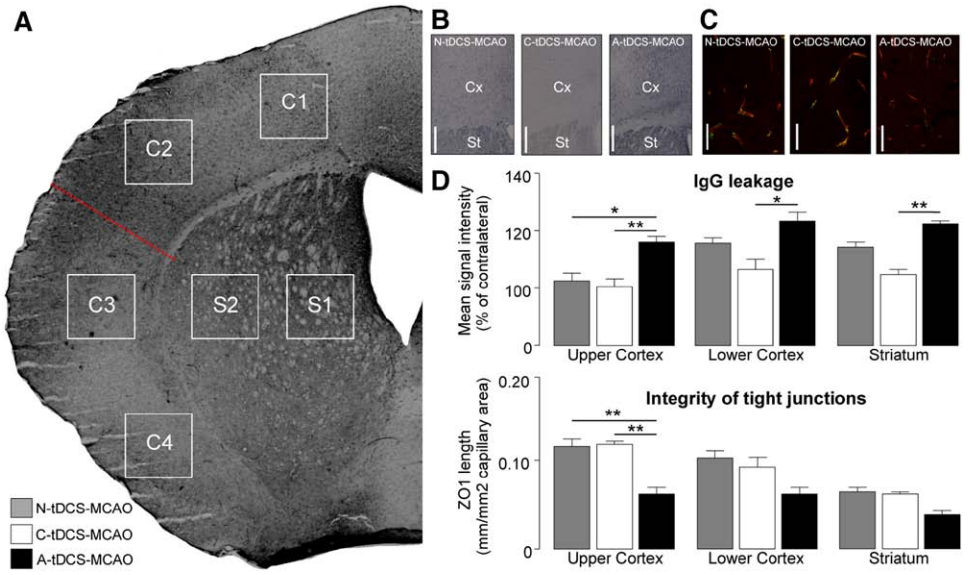

Figure 4. Postischemic blood brain barrier (BBB) dysregulation is amplified in mice that underwent anodal transcranial direct current after middle cerebral artery occlusion (A-tDCS-MCAO). **A**, Ischemic hemisphere from a representative A-tDCS-MCAO mouse, stained for IgG extravasation to assess BBB integrity; 2 upper cortical regions of interest (ROIs; C1–C2), 2 lower cortical ROIs (C3–C4), and 2 striatal ROIs (S1–S2) have been analyzed. Red dotted line represents the separation between upper and lower cortex. **B**, IgG stainings representative of each group of treatment. Scale bars, 500 μm. **C**, Representative confocal images of cortical Zona Occludens-1 (ZO1) coverage (green) over CD31 staining (red) in the ischemic cortex of treated mice. Scale bars, 100 μm. **D**, On quantitative analysis, A-tDCS-MCAO mice (black bars) displayed an increased extravasation of IgG compared with N-tDCS-MCAO (nonstimulated; gray bars) and C-tDCS-MCAO (cathodal; white bars) mice, occurring mostly in the upper cortical regions. Consistently, A-tDCS-MCAO mice showed a significant disruption of blood vessel tight junctions (ZO1 length per mm^2 over CD31$^+$ capillary surface) in upper cortical regions. Error bars in all panels indicate SEM, **P*<0.05, ***P*<0.01. Cx indicates ischemic cortex, and St, ischemic striatum.

mice (upper cortex and striatum, $P<0.01$; lower cortex, $P<0.05$; Figure 4B–4D).

Consistently, structural analysis of the endothelial tight junction protein Zona Occludens-1, which is fundamental in maintaining the BBB,[15] confirmed a significant treatment effect in the upper cortex ($H=9.63$; 2 d.f.; $P<0.01$). A-tDCS-MCAO mice displayed a significant lower coverage of Zona Occludens-1 over CD31$^+$ cortical blood vessels, with respect to both N-tDCS-MCAO ($P<0.01$) and C-tDCS-MCAO mice ($P<0.01$; Figure 4C and 4D).

A-tDCS Increases Early Postischemic Reperfusion and Late Hemorrhagic Transformation

Previous evidence has shown that A-tDCS is able to increase rCBF in both healthy human and rodents.[16,17] We thus assessed whether A-tDCS could influence early postischemic reperfusion (rCBF) values. No differences on rCBF were found before and during the induction of the MCAO in A-tDCS, C-tDCS, or N-tDCS-MCAO mice ($F_{2,72}=0.53$; $P=0.59$). However, during reperfusion a significant treatment effect on rCBF in the territory of the MCA was found ($F_{2,72}=2.273$; $P<0.0001$). Post hoc analysis revealed a significant increase of early reperfusion in A-tDCS-MCAO ($P<0.001$), compared with both C-tDCS-MCAO and N-tDCS-MCAO mice (Figure 5A). Considering the early postischemic reperfusion increase and the BBB structural and functional dysregulation induced by A-tDCS, we conducted a stereological analysis of cerebral bleedings. We observed a significant increase in the total number of hemorrhages ($H=7.03$; 2 d.f.; $P<0.05$) and total hemorrhagic area ($H=9.55$; 2 d.f.; $P<0.005$) in A-tDCS-MCAO mice if compared with both C-tDCS-MCAO ($P<0.01$) and N-tDCS-MCAO ($P<0.01$; Figure 5B). Cerebral bleedings were mostly found in brain areas located under the stimulating electrode, with remarkable differences among A-tDCS-MCAO, C-tDCS-MCAO, and N-tDCS-MCAO mice (Figure 5C and 5D). These data indicate that A-tDCS, in the acute phase of stroke, alters the structural and functional characteristic of the BBB, leading to hemorrhagic transformation.

Effects of tDCS When Delivered 4.5 Hours After MCAO

We finally sought to investigate whether C-tDCS had similar beneficial effects even if applied at later time points after ischemia. We applied the same 20′ on–20′ off–20′ on tDCS protocol starting 4.5 hours after the induction of 90-minute MCAO (Figure IIA in the online-only Data Supplement). We found that C-tDCS induced a functional amelioration of neurological deficits ($H=7.34$; 2 d.f.; $P<0.05$) evaluated at 24 hours postischemia, compared with N-tDCS-MCAO and A-tDCS-MCAO mice ($P<0.05$). The observed therapeutic effect of C-tDCS-MCAO was also paralleled by a slight reduction of the ischemic volume (C-tDCS-MCAO 42.57%±3.73 SEM; A-tDCS-MCAO 49.39%±1.89 SEM; n.s., and N-tDCS-MCAO 50.03%±2.35 SEM; n.s.) and a significant reduction of brain edema compared with A-tDCS-MCAO mice (C-tDCS-MCAO 31.86%±3.45 SEM; A-tDCS 48.33%±5.80 SEM; $P<0.05$, and N-tDCS-MCAO 37.68%±4.51 SEM; n.s.; Figure IIB and IIC in the online-only Data Supplement). Remarkably, we confirmed a significant increase in total hemorrhagic area ($H=8.36$; 2 d.f.; $P<0.05$) in A-tDCS-MCAO mice if compared

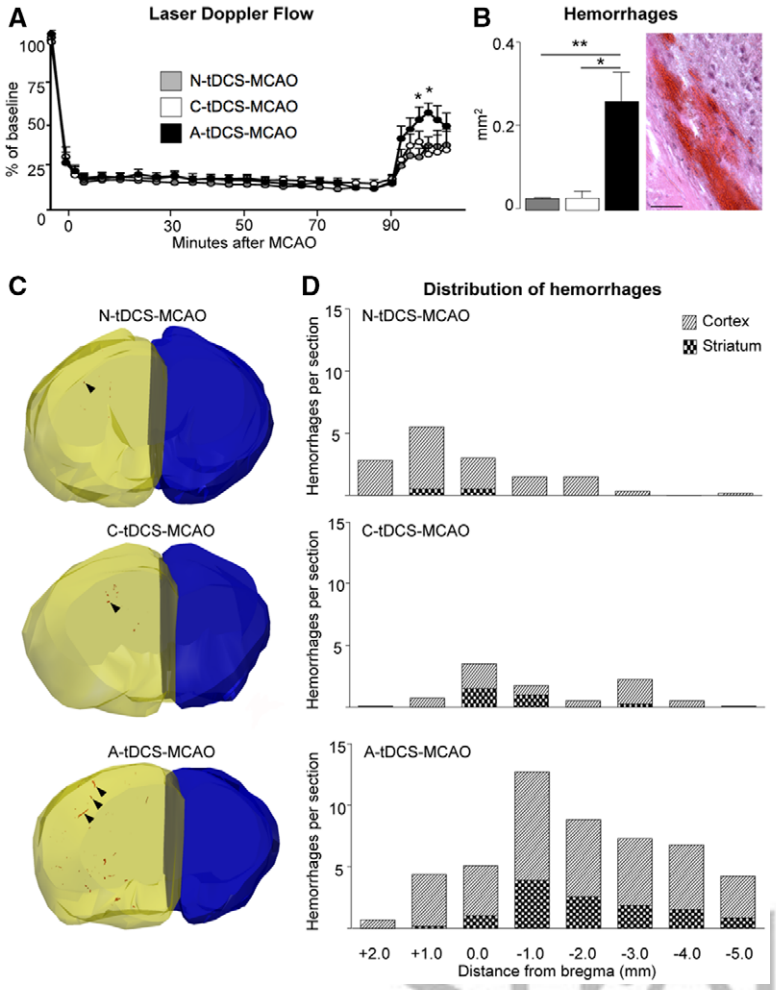

Figure 5. Anodal transcranial direct current stimulation (A-tDCS) increases postischemic reperfusion and favors hemorrhagic transformation. **A**, Laser Doppler Flow (LDF) recorded during the 90 minutes of middle cerebral artery occlusion (MCAO) and during the following reperfusion period. No differences were observed before and during MCAO among C-tDCS-MCAO (cathodal; white circles), N-tDCS-MCAO (nonstimulated; gray circles), and A-tDCS-MCAO mice (black circles). During early reperfusion, A-tDCS-MCAO displayed significant higher LDF values, compared with N-tDCS-MCAO and C-tDCS-MCAO mice. **B**, A-tDCS resulted in a significant increase of the total hemorrhagic area compared with both N-tDCS-MCAO and C-tDCS-MCAO mice. Gray bars represent N-tDCS-MCAO mice, white bars represent C-tDCS-MCAO mice, and black bars represent A-tDCS-MCAO mice. A representative hematoxylin–eosin stained section depicting a cortical hemorrhage of an A-tDCS-MCAO mouse is shown. Scale bar, 500 μm. **C**, Descriptive 3-dimensional reconstructions obtained from sequential sections analyzed for stereology of the contralateral healthy hemisphere (blue) and the ipsilateral whole ischemic hemisphere (yellow) for each group of treatment. Hemorrhages are depicted in red (arrowheads). **D**, Compared with N-tDCS-MCAO and C-tDCS-MCAO mice, A-tDCS-MCAO mice showed an increased number of hemorrhages in the cortex and striatum, mostly underneath the stimulating electrode. Dashed bars refer to the number of cortical hemorrhages per section; dotted bars refer to the number of striatal hemorrhages per section. Error bars in all panels indicate SEM, **P*<0.05, ***P*<0.01, ****P*<0.001.

with both C-tDCS-MCAO ($P<0.01$) and N-tDCS-MCAO ($P<0.05$; Figure IID in the online-only Data Supplement).

Discussion

Our data show for the first time a protective effect of C-tDCS if applied in the very early stage of experimental ischemic stroke. As already observed in human studies,[11,18] C-tDCS was able to lower cortical glutamate in our mice. This effect could be due, at least in part, to a decreased rate of glutamate synthesis subsequent to spontaneous neuronal firing modulation.[19] Interestingly, we also found a lower level of alanine in C-tDCS-treated mice, which correlates with glutamate levels and may be suggestive of an increased conversion of glutamate into glutamine.[20] These findings were corroborated by a striking downregulation of NR2B in C-tDCS-sham mice, suggesting that C-tDCS might be able to reduce the overall cortical glutamate activity, through the modulation of NMDAR. Previous findings showed indeed that NMDAR antagonists play a major role in attenuating most of tDCS cortical effects both in vivo[21] and in vitro.[22] Compared with other NMDAR subunits, NR2B preferentially contributes to pathological processes linked to overexcitation of glutamatergic pathways, representing an ideal target for neuroprotection.[23,24] As a matter of fact, in mature cortical cultures and in rats subjected to brain ischemia, activation of either synaptic or extrasynaptic NR2B-containing NMDARs results in excitotoxicity and neuronal apoptosis.[25]

The ability of short pulses of C-tDCS to lower the excess of cortical glutamate in healthy mice prompted us to explore whether or not such stimulation protocol might have a neuroprotective role in the very early phase of ischemic stroke, which is characterized by overt glutamatergic excitotoxicity.[12] We thus tested our protocol in mice undergoing 90-minute MCAO. C-tDCS was able to induce a sustained reduction of ischemic stroke volume ≤3 days postischemia when applied in the very early phase of MCAO and, although to a lesser extent, also when applied ≤4.5 hours poststroke. As a consequence, clinical deficits were significantly improved and functional preservation of the cortical and descending motor pathways (assessed with RMT) was observed. Consistently, we also found that C-tDCS was able to preserve the viability of cortical neurons, as a reduced number of Caspase3$^+$ apoptotic neuronal cells was found in the cortex of C-tDCS-MCAO-treated mice compared with A-tDCS-MCAO and N-tDCS-MCAO mice. The role of tDCS in early stages of ischemic stroke was further explored by measuring the inflammatory reaction occurring in response to ischemia. It is known that ischemic neurons produce discrete amounts of tumor necrosis factor-α, a cytokine that can further exacerbate the ischemic damage by activating microglia.[26] Additionally, glutamate per se might also exert

a pivotal role in triggering microglia activation.[27] Whatever the triggering factor, activated microglia produce neurotoxins, including nitric oxide and reactive oxygen species, that worsen ischemic tissue damage.[28] Indeed, C-tDCS-MCAO mice showed a lower amount of cortical Iba1$^+$ cell infiltration compared with A-tDCS-MCAO and N-tDCS-MCAO mice, and a lower amount of cortical glutamate with a proportional decrease in taurine.[29] This finding might be attributed to the fact that the neuroprotective effect exerted by C-tDCS in the early phase of stroke also protects and reduces secondary injury mechanisms, such as the postischemic inflammatory reaction sustained by activated microglia.[30] Nevertheless, we cannot exclude that our results might be also due, at least in part, to the ability of C-tDCS to reduce cortical-spreading depressions,[31,32] a major mechanism of acute ischemic damage induced by glutamate excitotoxicity. The reduced levels of creatine after stroke in C-tDCS-MCAO mice copes with this hypothesis, because this metabolite has been associated with the electric silencing of the ischemic penumbra.[33] Because the altered metabolic balance is one of the main detrimental mechanisms of acute ischemic stroke, it could be also argued that C-tDCS exerts its neuroprotective role by reducing brain metabolism in ischemic regions.

Despite previous data on the positive effects of A-tDCS in the subacute phase after cerebral ischemia (1 day and 1 week after MCAO),[34] we found that A-tDCS in the very acute phase of ischemic stroke was ineffective in inducing a functional amelioration. Although this apparent discrepancy might be simply explained by the different timing and current density (2.8 versus 5.5 mA/cm^2) of the 2 protocols, we favor attributing the detrimental consequences of acute A-tDCS to the alterations induced by the stimulation on vascular tone and BBB integrity. The observed facilitation of early reperfusion on filament withdrawal in A-tDCS-MCAO mice is in line with previous reports showing that A-tDCS is able to increase rCBF in cortical regions by modulating cerebral vessels.[16] Because vascular and neuronal functions in the brain are closely interrelated into the brain, changes in blood perfusion during tDCS could be consistent with a primary neuronal action via neurovascular coupling.[17] However, supporting evidence suggests a direct effect of tDCS on vascular response.[35] Additionally, endothelial cell cultures, including models of the BBB, can be electrically stimulated and high-intensity electric stimulation was shown to increase transport across this model through a phenomenon defined as electropermeation.[36] Indeed we found that A-tDCS had major effects on vasodynamic changes (increased postischemic reperfusion) and BBB structural and functional integrity in our mouse model of cerebral ischemia.

Despite increased reperfusion might be interpreted as beneficial in some cases, the observed detrimental behavioral and neuropathological outcomes in A-tDCS-MCAO mice suggests that early hyperreperfusion might represent a detrimental early hyperemia.[37] In fact, although restoration of oxygen and glucose supply reinstates the oxidative phosphorylation that helps normalizing energy after reperfusion, a parallel cascade of deleterious biochemical processes can also antagonize the beneficial effect of early reperfusion.[38] It has been variably reported that oxygen consumption might decrease during hyperemia despite an increased blood flow in the hyperemic areas.[37] As a matter of fact, cerebral autoregulation, which usually provides dynamic protection to the brain from excessive perfusion, is often impaired after ischemic stroke due to the early release of nitric oxide (and free radicals) damaging cerebrovascular endothelium, thus inducing vasodilatation and increased cerebral vessel permeability.[39,40]

BBB disruption results in albumin and high-molecular-weight proteins extravasation. Accordingly, A-tDCS, but not C-tDCS, increased the extravasation of IgG from circulating blood and reduced blood vessel tight junctions. Therefore, the increased number of hemorrhages observed in A-tDCS-MCAO mice might be attributed to these latter findings and to the abovementioned increased reperfusion. Although increased blood flow induced by A-tDCS might be beneficial in subacute and chronic stroke, the present data point out that our acute stroke setting is rather detrimental as it leads to increased BBB dysfunction, increased edema, and ischemic lesion volume. In addition to its effects on BBB integrity and vascular tone, oxidative damage is also responsible for delayed tissue damage, apoptosis, and inflammation after acute ischemic stroke.[41] Indeed, we found that A-tDCS applied during MCAO induced an increased number of cortical Caspase3$^+$ cells compared with N-tDCS-MCAO mice (which did not preferentially affect neuronal or endothelial cell apoptosis), an increase of final ischemic volume, as well as a dramatic increase of blood-borne, central nervous system-infiltrating inflammatory CD45$^+$ and MPO$^+$ cells. Consistently, we found that A-tDCS induced an increase of brain edema and hemorrhagic transformation, also when administered 4.5 hours after MCAO.

Despite the mechanisms of tDCS in stroke are far from being fully understood, our study supports the use of cathodal tDCS in the hyperacute phase of ischemic stroke, although indicating a possible hazardous effects of A-tDCS in the very same phase. It is reasonable to think that different polarities of tDCS could have a Janus-like role in the ischemic brain, depending on the timing, site of application, and pathophysiological milieu. Nevertheless, when appropriately tuned, tDCS in acute stroke is a promising therapeutic strategy because of its low costs, fast administration, and ease of delivery to brain cortical areas, regardless of blood perfusion.

Acknowledgments

Study conception: Dr Leocani; study design: Drs Peruzzotti-Jametti, Cambiaghi, Bacigaluppi, Comi, Musco, Martino, and Leocani; data collection: Dr Peruzzotti-Jametti, Dr Cambiaghi, M. Gallizioli, E. Gaude, Dr Mari, S. Sandrone, and Dr Teneud; data analysis: Dr Peruzzotti-Jametti, Dr Cambiaghi, Dr Bacigaluppi, E. Gaude, Dr Mari, S. Sandrone, and Dr Martino; data interpretation and article writing: Drs Peruzzotti-Jametti, Cambiaghi, Bacigaluppi, Comi, Musco, Martino, and Leocani.

Sources of Funding

Joint Italian–Israeli laboratory on Brain modulation in neuroimmune, neurodegenerative, and mental disorders (Italian Ministry of Foreign Affairs), TargetBrain (EU Framework 7 project HEALTH-F2-2012–279017), and NEUROKINE (EU Framework 7 ITN project).

Disclosures

None.

References

1. Fregni F, Pascual-Leone A. Technology insight: noninvasive brain stimulation in neurology-perspectives on the therapeutic potential of rTMS and tDCS. *Nat Clin Pract Neurol*. 2007;3:383–393.
2. Priori A. Brain polarization in humans: a reappraisal of an old tool for prolonged non-invasive modulation of brain excitability. *Clin Neurophysiol*. 2003;114:589–595.
3. Webster BR, Celnik PA, Cohen LG. Noninvasive brain stimulation in stroke rehabilitation. *NeuroRx*. 2006;3:474–481.
4. Schlaug G, Renga V, Nair D. Transcranial direct current stimulation in stroke recovery. *Arch Neurol*. 2008;65:1571–1576.
5. Kim SJ, Kim BK, Ko YJ, Bang MS, Kim MH, Han TR. Functional and histologic changes after repeated transcranial direct current stimulation in rat stroke model. *J Korean Med Sci*. 2010;25:1499–1505.
6. Baba T, Kameda M, Yasuhara T, Morimoto T, Kondo A, Shingo T, et al. Electrical stimulation of the cerebral cortex exerts antiapoptotic, angiogenic, and anti-inflammatory effects in ischemic stroke rats through phosphoinositide 3-kinase/Akt signaling pathway. *Stroke*. 2009;40:e598–e605.
7. Hermann DM, Chopp M. Promoting brain remodelling and plasticity for stroke recovery: therapeutic promise and potential pitfalls of clinical translation. *Lancet Neurol*. 2012;11:369–380.
8. Peruzzotti-Jametti L, Bacigaluppi M, Sandrone S, Cambiaghi M. Emerging subspecialties in Neurology: transcranial stimulation. *Neurology*. 2013;80:e33–e35.
9. Nitsche MA, Paulus W. Excitability changes induced in the human motor cortex by weak transcranial direct current stimulation. *J Physiol*. 2000;527 pt 3:633–639.
10. Cambiaghi M, Velikova S, Gonzalez-Rosa JJ, Cursi M, Comi G, Leocani L. Brain transcranial direct current stimulation modulates motor excitability in mice. *Eur J Neurosci*. 2010;31:704–709.
11. Stagg CJ, Best JG, Stephenson MC, O'Shea J, Wylezinska M, Kincses ZT, et al. Polarity-sensitive modulation of cortical neurotransmitters by transcranial stimulation. *J Neurosci*. 2009;29:5202–5206.
12. Dirnagl U, Iadecola C, Moskowitz MA. Pathobiology of ischaemic stroke: an integrated view. *Trends Neurosci*. 1999;22:391–397.
13. Liebetanz D, Koch R, Mayenfels S, König F, Paulus W, Nitsche MA. Safety limits of cathodal transcranial direct current stimulation in rats. *Clin Neurophysiol*. 2009;120:1161–1167.
14. Liu Y, Wong TP, Aarts M, Rooyakkers A, Liu L, Lai TW, et al. NMDA receptor subunits have differential roles in mediating excitotoxic neuronal death both in vitro and in vivo. *J Neurosci*. 2007;27:2846–2857.
15. Armulik A, Genové G, Mäe M, Nisancioglu MH, Wallgard E, Niaudet C, et al. Pericytes regulate the blood-brain barrier. *Nature*. 2010;468:557–561.
16. Lang N, Siebner HR, Ward NS, Lee L, Nitsche MA, Paulus W, et al. How does transcranial DC stimulation of the primary motor cortex alter regional neuronal activity in the human brain? *Eur J Neurosci*. 2005;22:495–504.
17. Wachter D, Wrede A, Schulz-Schaeffer W, Taghizadeh-Waghefi A, Nitsche MA, Kutschenko A, et al. Transcranial direct current stimulation induces polarity-specific changes of cortical blood perfusion in the rat. *Exp Neurol*. 2011;227:322–327.
18. Clark VP, Coffman BA, Trumbo MC, Gasparovic C. Transcranial direct current stimulation (tDCS) produces localized and specific alterations in neurochemistry: a ^{1}H magnetic resonance spectroscopy study. *Neurosci Lett*. 2011;500:67–71.
19. Rothman DL, Sibson NR, Hyder F, Shen J, Behar KL, Shulman RG. In vivo nuclear magnetic resonance spectroscopy studies of the relationship between the glutamate–glutamine neurotransmitter cycle and functional neuroenergetics. *Philosop Trans R Soc B: Biol Sci*. 1999;354:1165–1177.
20. Dadsetan S, Bak LK, Sørensen M, Keiding S, Vilstrup H, Ott P, et al. Inhibition of glutamine synthesis induces glutamate dehydrogenase-dependent ammonia fixation into alanine in co-cultures of astrocytes and neurons. *Neurochem Int*. 2011;59:482–488.
21. Liebetanz D, Nitsche MA, Tergau F, Paulus W. Pharmacological approach to the mechanisms of transcranial DC-stimulation-induced after-effects of human motor cortex excitability. *Brain*. 2002;125(pt 10):2238–2247.
22. Fritsch B, Reis J, Martinowich K, Schambra HM, Ji Y, Cohen LG, et al. Direct current stimulation promotes BDNF-dependent synaptic plasticity: potential implications for motor learning. *Neuron*. 2010;66:198–204.
23. Zhang F, Guo A, Liu C, Comb M, Hu B. Phosphorylation and assembly of glutamate receptors after brain ischemia. *Stroke*. 2013;44:170–176.
24. Tymianski M. Emerging mechanisms of disrupted cellular signaling in brain ischemia. *Nat Neurosci*. 2011;14:1369–1373.
25. Picconi B, Tortiglione A, Barone I, Centonze D, Gardoni F, Gubellini P, et al. NR2B subunit exerts a critical role in postischemic synaptic plasticity. *Stroke*. 2006;37:1895–1901.
26. Barone FC, Arvin B, White RF, Miller A, Webb CL, Willette RN, et al. Tumor necrosis factor-alpha. A mediator of focal ischemic brain injury. *Stroke*. 1997;28:1233–1244.
27. Kaushal V, Schlichter LC. The utility of a new in vitro model of the stroke penumbra. *J Neurosci*. 2008;28:6537–6538.
28. Iadecola C. Bright and dark sides of nitric oxide in ischemic brain injury. *Trends Neurosci*. 1997;20:132–139.
29. Oja SS, Saransaari P. Modulation of taurine release in glucose-free media by glutamate receptors in hippocampal slices from developing and adult mice. *Amino Acids*. 2013;44:533–542.
30. Doyle KP, Simon RP, Stenzel-Poore MP. Mechanisms of ischemic brain damage. *Neuropharmacology*. 2008;55:310–318.
31. Liebetanz D, Fregni F, Monte-Silva KK, Oliveira MB, Amâncio-dos-Santos A, Nitsche MA, et al. After-effects of transcranial direct current stimulation (tDCS) on cortical spreading depression. *Neurosci Lett*. 2006;398:85–90.
32. Fregni F, Liebetanz D, Monte-Silva KK, Oliveira MB, Santos AA, Nitsche MA, et al. Effects of transcranial direct current stimulation coupled with repetitive electrical stimulation on cortical spreading depression. *Exp Neurol*. 2007;204:462–466.
33. Astrup J, Siesjö BK, Symon L. Thresholds in cerebral ischemia - the ischemic penumbra. *Stroke*. 1981;12:723–725.
34. Yoon KJ, Oh BM, Kim DY. Functional improvement and neuroplastic effects of anodal transcranial direct current stimulation (tDCS) delivered 1 day vs. 1 week after cerebral ischemia in rats. *Brain Res*. 2012;1452:61–72.
35. Malty AM, Petrofsky J. The effect of electrical stimulation on a normal skin blood flow in active young and older adults. *Med Sci Monit*. 2007;13:CR147–CR155.
36. Lopez-Quintero SV, Datta A, Amaya R, Elwassif M, Bikson M, Tarbell JM. DBS-relevant electric fields increase hydraulic conductivity of in vitro endothelial monolayers. *J Neural Eng*. 2010;7:16005.
37. Olsen TS, Larsen B, Skriver EB, Herning M, Enevoldsen E, Lassen NA. Focal cerebral hyperemia in acute stroke. Incidence, pathophysiology and clinical significance. *Stroke*. 1981;12:598–607.
38. Gürsoy-Ozdemir Y, Can A, Dalkara T. Reperfusion-induced oxidative/nitrative injury to neurovascular unit after focal cerebral ischemia. *Stroke*. 2004;35:1449–1453.
39. Janigro D, West GA, Nguyen TS, Winn HR. Regulation of blood-brain barrier endothelial cells by nitric oxide. *Circ Res*. 1994;75:528–538.
40. Eames PJ, Blake MJ, Dawson SL, Panerai RB, Potter JF. Dynamic cerebral autoregulation and beat to beat blood pressure control are impaired in acute ischaemic stroke. *J Neurol Neurosurg Psychiatry*. 2002;72:467–472.
41. Rodríguez-Yáñez M, Castellanos M, Blanco M, Mosquera E, Castillo J. Vascular protection in brain ischemia. *Cerebrovasc Dis*. 2006;21(2 suppl):21–29.

SUPPLEMENTAL MATERIAL

Supplemental Methods

Middle Cerebral Artery Occlusion (MCAO)

Five days after epicranial electrode implant, mice were weighted and anesthetized with 1.5% isoflurane (Merial, Assago, Italy) in 30% O_2 (remainder N_2O). Rectal temperature was maintained stable (36.5 ±0.5°C) by a feedback-controlled heating system (Harvard Instruments, Holliston, MA, USA). Laser Doppler Flow (LDF) was monitored by means of a flexible 0.5 mm fiber optic probe (Perimed, Stockholm, Sweden) attached to the intact skull overlying the core region of the middle cerebral artery territory. Focal cerebral ischemia was induced with a silicon-coated (Xantopren, Bayer Dental, Osaka, Japan) 8-0 nylon filament (Ethilon, Ethicon, Norderstedt, Germany) that was inserted into the left common carotid artery and was advanced through the internal carotid artery to the origin of the middle cerebral artery, as previously described.[1] Following 90' of MCAO, reperfusion was initiated by withdrawing the filament. Continuous measures of rCBF were recorded during the experiment. The initial drop and the average flow during ischemia (90') and reperfusion (15') were calculated as a percentage of the baseline (10'), prior to MCA occlusion. In all groups, laser Doppler flow values dropped after MCAO to 20% of baseline values in the territory supplied by the ipsilateral Middle Cerebral Artery. After surgery, wounds were carefully sutured, anesthesia was discontinued and mice were put back in their cages to allow recovery. To correct fluid loss during the surgical intervention, 0.5 ml of sterile isotonic saline (0.9% NaCl) was intra-peritoneally injected in each animal.

Transcranial Direct Current Stimulation

Epicranial electrode implant was carried out in mice under 2% isoflurane anesthesia (Merial, Assago, Italy) maintained at a stable temperature (36.5 ±0.5°C) using a feedback-controlled heating system (Harvard Instruments, Holliston, MA, USA). The scalp and underlying tissues were removed and the epicranial electrode was implanted using glass ionomer dental cement (Ketac Cem, ESPE Dental AG, Seefeld, Germany). The center of the active electrode (radius 1,2 mm) was positioned over the left parietal area, 2.5 mm left and 0.5 mm posterior to the bregma (Supplemental Figure 1B). The counter electrode was a saline-soaked sponge applied over the ventral thorax (5.2 cm^2). Epicranial implanted electrode was filled with saline solution (0.9% NaCl) just prior to stimulation, as previously described.[2] tDCS was applied at current intensity of 250 μA by a constant current stimulator; this resulted in a current density of 5.5 mA/cm^2. Mice with real or sham MCAO underwent tDCS starting 30' (or 4,5 hours) after the onset of the procedure (MCAO or anesthesia, respectively) for 20', followed by 20' rest and additional 20' tDCS, for a total of 40' stimulation in 1 hour. For animals undergoing real tDCS, the current intensity was ramped up and down for 10 seconds instead of switching it on and off directly, in order to avoid a stimulation break effect.[3] The non-stimulated mice underwent the same procedure of stimulated groups, but no current was applied.

Motor evoked potentials and behavioral outcome

Right forelimb resting motor threshold (RMT) upon electrical stimulation was measured 3 days before MCAO (baseline) in all animals subjected to MCAO. A subgroup of 18 animals (N-tDCS-MCAO n=6; C-tDCS-MCAO n=6; A-tDCS-MCAO n=6) was randomly selected for RMT at 24 hours after ischemia. Modified Neurologic Severity Score (mNSS)[4] was assessed on those mice and on mice that were allowed to live up to 72 hours post-ischemia. RMT was measured using the same stimulation montage adopted for tDCS, as previously described.[2] The electromyographic signal was recorded using the System-Plus software (Micromed, Mogliano Veneto, Italy) at sweep velocity of 20 ms with a sensitivity of 500 μV

(12 bit). The bandpass filter was set at 50 Hz–5 kHz. The active needle electrode (S.E.I., Cittadella, Italy) was inserted into the center of the contralateral forelimb footpad and the reference needle under the skin of the second digit, at a distance of about 3–4 mm from the recording electrode. Square wave current pulses of 50 μs width were applied at a frequency of 0.5 Hz. RMT was determined as the lowest current intensity (mA) that allowed the recording of at least three out of six responses of amplitude greater than 50 μV from consecutive stimulation trials in the recorded muscle.[2]

Evaluation of ischemic damage and neuroinflammation

Twenty-four and seventy-two hours after MCAO animals were weighted, deeply anesthetized and transcardially perfused with 25mL of saline phosphate buffer (PBS: 0.1 M, pH 7.2) with EDTA 0.5 M, followed by 25mL of paraformaldehyde (4% in PBS). Brains were carefully dissected, postfixed overnight and embedded in tissue-freezing medium for cryostat sectioning. Coronal 30 μm-thick sections were then cut serially, collecting one section every 20 on the same slide for stereological analyses. For the measurement of the total ischemic volume and cerebral oedema index, sections (n=10-12 sections per mouse) were stained with Fluoro-Jade-B (Histo-Chem Inc. Jefferson AR).[5] Brain slices were analyzed using a Stereo Investigator v 3.0 software (MicroBrightField, Inc., Colchester, VT, USA) and descriptive 3D reconstructions were obtained. The volume of infarction was measured by the 'indirect method', which corrects for brain edema.[6] Data were expressed as percentage values of the infarcted vs. contralateral intact hemisphere. The edema index was calculated by subtracting the total volume of the ischemic from the non-ischemic hemisphere and expressed as percentage of contralateral hemisphere. Using brain sections from the same animals, immunohistochemistries for quantification of apoptosis and neuroinflammation were performed using rat anti-CD31 (1:100, BD Biosciences, San Jose, CA USA), rabbit anti-cleaved Caspase3 (1:100; Cell Signalling, Danvers, MA USA), mouse anti-NeuN (1:500, Chemicon, Darmstadt Germany), rabbit anti-Iba1 (1:250; Wako, Osaka Japan), rat anti-CD45 (1:100; BD Biosciences) and rabbit anti-myeloperoxidase (MPO) (1:200, DAKO, Glostrup, Denmark) as primary antibodies. For sections stained with biotinylated antibodies, endogenous peroxidase activity was blocked with avidin/biotin blocking kit (Vector laboratories, Burlingame, CA, USA) and stained with Vectastain®AB kit (Vector laboratories), followed by the liquid DAB+ Substrate (DAKO). Appropriate anti-rat and anti-rabbit fluorophore- (Alexa-fluor 488, 546; Molecular Probes, Carlsbad, CA, USA) or biotin- (Amersham) conjugated secondary antibodies were used.[7] Nuclei were counter labeled with 4'-6-diamidino-2-phenylindole (DAPI) (Roche). Immunofluorescence stainings were evaluated with a CCD camera (DC 480, Leica, St. Gallen, Switzerland) under a fluorescence microscope (Olympus, BX51) and photographs of equally distanced regions of interest (ROI) on a 40X objective lens were collected in the peri-ischemic cortex (n=4 ROI) and striatum (n=2 ROI). The number of $Caspase3^+$, $Iba1^+$ and $CD45^+$ cells was normalized over the total number of $DAPI^+$ cells and then averaged in the cortex and in the striatum (n=3 sections per mouse; n=6 randomly selected mice per group). The density of MPO^+ cells (number of cells per mm^2) was calculated with the Neurolucida software (20X objective lens) in the upper and lower ipsilateral cortical areas (see Figure 4A) and in the ipsilateral ischemic striatum. Data was averaged on 3 biotinylated sections per mouse (n=6 randomly selected mice per group).

Assessment of BBB integrity and hemorrhages

Immunoglobulin G (IgG) extravasation was determined using standard immunohistochemistry and avidin-peroxidase reaction. Endogenous peroxidase activity was blocked with avidin/biotin blocking kit (Vector Laboratories) and anti-mouse IgG biotin-conjugated secondary antibody made in goat (1:500; BD Biosciences) was used. Sections

were immersed with Vectastain®AB kit (Vector Laboratories) and revealed with Diamino Benzidine Tetrahydrochloride (DAB) (DAKO). Three adjacent 30µm coronal sections for each brain were processed for IgG extravasation assay.[8] Optical density (OD) was assessed through ImageJ software (NIH, USA): the minimum IgG extravasation results in black (OD value=0), whereas the maximum IgG extravasation results in white (OD value=255). IgG extravasation is showed as percentage of OD of ipsilateral lesioned hemisphere over OD of contralateral healthy hemisphere. Zona Occludens 1 (ZO1) coverage over CD31 expression was assessed on immunofluorescence stainings performed using a rat anti-CD31 (1:100, BD Pharmigen), a mouse anti-ZO-1 FITC (1:200, Invitrogen), as primary antibodies, and fluorophore-conjugated 546 goat anti-rat and 488 goat anti-mouse as secondary antibodies (1:000; Alexa-fluor Molecular Probes). Length of ZO1 was measured using the Neuro J plug-in of ImageJ software and expressed in µm over the area of the corresponding $CD31^+$ capillary, as previously described.[9] Both IgG and ZO1/CD31 stainings were evaluated under a bright field/fluorescence microscope (Olympus, BX51) and six regions of interest (ROI) were created (see Figure 4A). Photographs of equally distanced ROI on a 20X objective lens were collected in the upper cortex (n=2 ROI), lower cortex (n=2 ROI) and in the striatum (n=2 ROI) of both ipsilateral and contralateral hemispheres (n=3 sections per mouse; n=6 randomly selected mice per group). Hemorrhages were evaluated as extravasation of erythrocytes on hematoxylin and eosin stained sections (n=10-12 sections per mouse; n=6 randomly selected mice per group) (Figure 5B). Number of hemorrhages, single hemorrhagic areas, as well as descriptive 3D reconstructions, were assessed by drawing the corresponding contours on a 63X objective lens with Neurolucida v 3.0 software (MicroBrightField, Inc., Colchester, VT, USA). Total hemorrhagic area was calculated as the sum of single hemorrhagic areas on every section for each mouse.

NMR spectroscopy

For NMR spectroscopy (NMRs), animals were sacrificed immediately after the 90' MCAO (N-tDCS-MCAO n=3; C-tDCS-MCAO n=3; A-tDCS-MCAO n=3) or the sham procedure (C-tDCS-sham n=4; A-tDCS-sham n=4; N-tDCS-sham n=4). Mice were decapitated and brains were quickly removed and put into dry ice for subsequent NMR analysis. Frozen brains were dissected in order to isolate the parenchyma underneath the stimulating electrode (ipsilateral cortex) and homotopic areas (contralateral cortex). Metabolic tissue extracts were obtained by methanol/chloroform/water extraction protocol, as previously described.[10] For NMR spectra acquisitions, lyophilized polar metabolites were resuspended in 225 µl of bi-distilled water (ddH2O) and mixed with 20 µl of deuterated PBS solution containing DSS, plus 5 µl of 1.2% NaN3 water solution. Final sample volume was 250 µl with 50 mM PBS, pH 7, 0.02% NaN3 and 90 µM DSS. These solutions were loaded into 3 mm NMR tubes (Wilmad LabGlass) and then introduced into NMR spectrometer. NMR spectra were acquired on a 600 MHz spectrometer (Bruker Avance 600 Ultra Shield TM Plus, Bruker BioSpin) equipped with a triple-resonance TCI cryoprobe with a z shielded pulsed-field gradient coil. All experiments were carried out at 302 K, spectrometer temperature was calibrated using pure methanol-d4 sample. Sample temperature inside the spectrometer was equilibrated for 5 min before each spectrum acquisition. For each sample, noesy Bruker pulse sequence were used for 1D-1H spectra acquisition. To facilitate metabolite identification 2D J-resolved, 2D 1H-1H-TOCSY and 2D 1H-13C-HSQC spectra were acquired. Molecular identification and assignment of compounds were performed by using CCPNmr Metabolomics project and ChenoMX NMR Suite, demo version.

Western blot analysis of cortical tissue

Immediately after the 90' sham MCAO procedure and tDCS application, brains were rapidly removed after decapitation and the cortex was dissected. To obtain synaptosome preparation, the cortical tissue of two mice for each experimental condition was pooled and homogenized in 1 ml of homogenization buffer (10 mM Tris HCl pH7.4, 260 mM sucrose and cocktail of protease inhibitors, Sigma). Homogenate was centrifuged at 1000 x g at 4°C for 10 min to remove nuclei and cell debris. The resulting supernatant was centrifuged at 12'500 x g at 4°C for 20 min. Pellet was suspended in 160 µl of homogenization buffer and used for western blot analysis. Total proteins in the synaptosome preparation were quantified by using BCA kit (Pierce, Thermo Scientific IL 61101 USA) and 50 µg of each sample were applied to a SDS-PAGE and western blotting was performed. The blots were incubated overnight at 4°C with the following antibodies: rabbit anti-Glutamate Receptor NMDAR1 (NR1, 116 kDa) (1:2000; Sigma), rabbit anti-Glutamate Receptor NMDAR2B (NR2B, 180 kDa) (1:1000; Millipore), and mouse anti-β-Actin (42 kDa) (1:30000; Sigma). Secondary antibodies coupled with HRP (Biorad, UK) were then used. The immunoreactivity was visualized by using the ECL detection system (Millipore). Gel images were acquired using a Molecular Dynamics Personal Densitometer (Amersham Biosciences, USA) and processed by using the ImageQuant software (Amersham Biosciences). Densitometries were then normalized over the corresponding housekeeping gene β-Actin (C-tDCS-sham n=8; A-tDCS-sham n=8; N-tDCS-sham n=8).

Statistics

Statistical analyses were performed with GraphPad Prism (version 5.00 for Windows, GraphPad Software, San Diego California USA). Histological outcomes, functional assessments and densitometries were analyzed using nonparametric Kruskal-Wallis test followed by Mann-Whitney-Wilcoxon test. To test for differences in rCBF, a two-way ANOVA analysis, followed by Tukey post-test, was performed. For 1D-1H NMR spectra statistical interpretation absolute concentrations of metabolites were calculated by referencing with internal standard and were then subject to both multivariate and univariate statistical analyses. In order to identify patterns of variation induced by tDCS treatments, principal component analysis (PCA) was performed as exploratory technique. A decisional tree algorithm was also used for performing univariate tests: Shapiro Wilk's test for normality was performed on each metabolite distribution and, depending on the results from such test, Welch's T test or Wilcoxon-Mann-Whitney test were applied. Ratio of absolute concentrations of metabolites between non-stimulated, C-tDCS and A-tDCS mice was also calculated. Both multivariate and univariate statistical interpretations were carried out using the R package MUMA Values are given in the text as mean SEM. $P<0.05$ was accepted as significant.

References

1. Bacigaluppi M, Pluchino S, Peruzzotti-Jametti L, Kilic E, Kilic U, Salani G, et al. Delayed post-ischaemic neuroprotection following systemic neural stem cell transplantation involves multiple mechanisms. *Brain*. 2009;132:2239–2251.

2. Cambiaghi M, Velikova S, Gonzalez-Rosa JJ, Cursi M, Comi G, Leocani L. Brain transcranial direct current stimulation modulates motor excitability in mice. *European Journal of Neuroscience*. 2010;31:704–709.

3. Liebetanz D, Fregni F, Monte-Silva KK, Oliveira MB, Amâncio-dos-Santos Â, Nitsche MA, et al. After-effects of transcranial direct current stimulation (tDCS) on cortical spreading depression. *Neuroscience Letters*. 2006;398:85–90.

4. Chen J, Zhang C, Jiang H, Li Y, Zhang L, Robin A, et al. Atorvastatin induction of VEGF and BDNF promotes brain plasticity after stroke in mice. *J Cereb Blood Flow Metab*. 2005;25:281–290.

5. Schmued LC, Hopkins KJ. Fluoro-Jade B: a high affinity fluorescent marker for the localization of neuronal degeneration. *Brain Research*. 2000;874:123–130.

6. Lin TN, He YY, Wu G, Khan M, Hsu CY. Effect of brain edema on infarct volume in a focal cerebral ischemia model in rats. *Stroke*. 1993;24:117–121.

7. Pluchino S, Zanotti L, Rossi B, Brambilla E, Ottoboni L, Salani G, et al. Neurosphere-derived multipotent precursors promote neuroprotection by an immunomodulatory mechanism. *Nature*. 2005;436:266–271.

8. Elali A, Doeppner TR, Zechariah A, Hermann DM. Increased blood–brain barrier permeability and brain edema after focal cerebral ischemia induced by hyperlipidemia. *Stroke*. 2011;42:3238-3244

9. Bell RD, Winkler EA, Sagare AP, Singh I, LaRue B, Deane R, et al. Pericytes control key neurovascular functions and neuronal phenotype in the adult brain and during brain aging. *Neuron*. 2010;68:409–427.

10. Wu H, Southam AD, Hines A, Viant MR. High-throughput tissue extraction protocol for NMR- and MS-based metabolomics. *Anal. Biochem.* 2008;372:204–212.

Supplemental figures

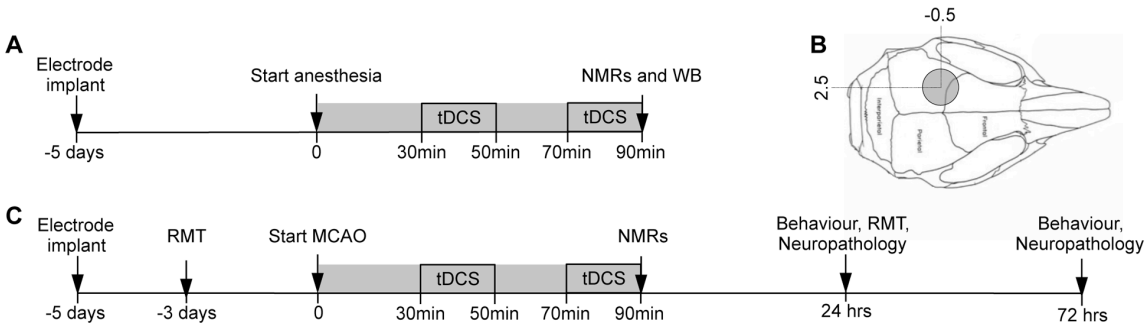

Supplemental Figure I. (**A**) Experimental paradigm for tDCS studies on healthy mice. A transcranial direct current stimulation protocol consisting of 20'on - 20'off - 20'on of either cathodal tDCS (C-tDCS-sham) or anodal-tDCS (A-tDCS-sham) was applied to healthy mice (the control group remained non-stimulated: N-tDCS-sham). Nuclear Magnetic Resonance spectroscopy (NMRs) and Western blot analyses were performed at the end of two 20' pulses of tDCS, as indicated. (**B**) Transcranial direct current stimulation was applied through an epicranial electrode (inner area, 4.5 mm^2) implanted 5 days before tDCS over the left parietal area (2.5 mm left and 0.5 mm posterior to the bregma) of healthy and MCAO mice. (**C**) Experimental paradigm for tDCS studies on MCAO mice. Mice were treated with a tDCS protocol consisting of 20'on - 20'off - 20'on of either cathodal tDCS (C-tDCS-MCAO) or anodal-tDCS (A-tDCS-MCAO) (the control group remained non-stimulated: N-tDCS-MCAO), starting 30 minutes after MCAO. NMR spectroscopy was performed at the end of the two 20' pulses of tDCS. RMT was assessed at 24 hours after MCAO. Behavioral assessment and neuropathology were conducted up to 72 hours after MCAO.

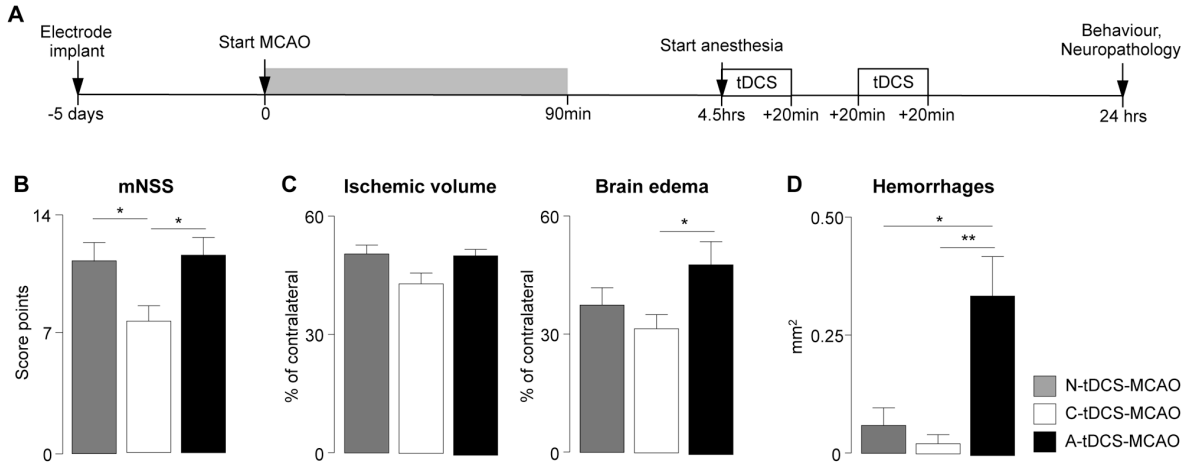

Supplemental Figure II. C-tDCS improved functional outcome if administered up to 4,5 hours post-ischemia. (**A**) Mice were treated with the same tDCS protocol starting 4,5 hours after MCAO, behavioral assessment and neuropathology were conducted at 24 hours after MCAO. (**B**) C-tDCS-MCAO mice (white bars) showed less disability at 24 hours post ischemia, evaluated with the mNSS (modified-Neurological-Severity-Score), compared to both N-tDCS-MCAO (grey bars) and A-tDCS-MCAO mice (black bars). (**C**) C-tDCS induced a small reduction of the ischemic volume compared to both N-tDCS-MCAO and A-tDCS-MCAO mice, while it significantly reduced brain edema compared to A-tDCS-MCAO mice. (**D**) A-tDCS resulted in a significant increase of the total hemorrhagic area compared to both N-tDCS-MCAO and C-tDCS-MCAO mice. Grey bars represent N-tDCS-MCAO mice, white bars represent C-tDCS MCAO mice and black bars represent A-tDCS-MCAO mice. Error bars in all panels indicate SEM, *$p<0.05$, **$p<0.01$.

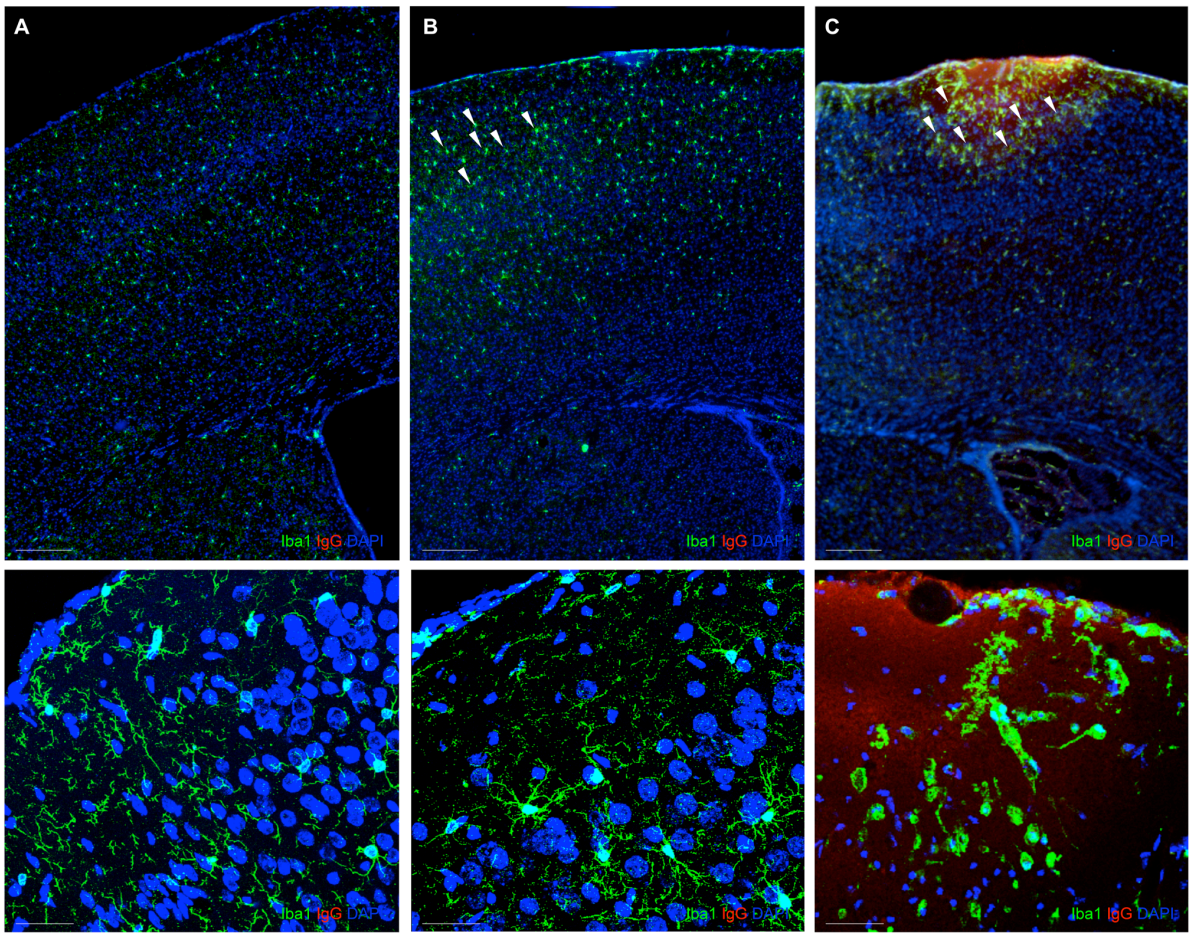

Supplemental Figure III. Transcranial direct current stimulation protocols were initially tested on healthy mice. Mice were subjected to 1 hour (**A**), 2 hours (**B**) and 4 hours (**C**) of C-tDCS to verify any possible damage induced by the current per se. One hour of continuous stimulation did not produce any observable lesion or pathological changes. Conversely, two hours of C-tDCS induced a selective accumulation of Iba1+ cells (green) within the stimulated cortex (arrowheads in **B**). Four hours of C-tDCS induced marked microglial activation (arrowheads in **C**) and IgG (red) extravasation (scale bars 125 μm). Lower microphotographs in each panel were acquired with a 40X lens (scale bars 50 μm). Nuclei are counterstained with DAPI (blue).